

Physical seismic modelling of anisotropic wave propagation: Latest results and future directions

R.J. Brown, D.C. Lawton, S.P. Cheadle and G.B. Marchisio

ABSTRACT

In this paper we report the results of continued scaled physical model experiments in the laboratory wherein ultrasonic elastic waves are propagated through an anisotropic medium of orthorhombic symmetry. Whereas earlier experiments consisted for the most part in sending and receiving on opposite faces of a small cube of the phenolic material, the results at hand are from multiple-offset profiles run parallel and at 45 degrees to principal directions on a larger slab of phenolic.

The variation of NMO (or stacking) velocity with offset (or angle of incidence) has been determined for compressional and transverse shear waves for the two principal directions on the 3-face (parallel to laminations) of the slab. These velocities are compared with the corresponding values calculated from Thomsen's approximate equations. The two sets of velocity values agree quite well, maximum differences being less than 1% for qP and about 2% for qSH.

Shot records were acquired for a variety of source and receiver polarizations, initially for profiles along principal directions. These records, for which there is sagittal symmetry, do not display any fundamental differences to records acquired over transversely isotropic media. The effect of the shear-wave window and the variation of the hyperbolic NMO parameter with offset are clearly seen. For profiles shot at 45 degrees to principal directions, we see clear shear-wave splitting at and near zero offset. In addition, we see more complicated wave effects, such as one or another wave phase dying out with increasing offset, which could be due to cusping of wave surfaces or rapid changes of amplitude and/or polarization with ray direction, consequences of nearby shear-wave singularities.

INTRODUCTION

Using as a medium the anisotropic phenolic laminate described by Cheadle et al. (1990), hereafter referred to as Paper 1, physical seismic experimentation has been continuing in the laboratory with scaled-down models (typically 1:5000) and scaled-up frequencies (typically 5000:1). In Paper 1 we looked primarily at body waves propagating along principal (or symmetry) directions, corresponding to zero-offset shot records on each of three principal faces (symmetry planes) of the phenolic. The only departure from this simplest case, necessary to enable determination of the nine stiffnesses of the material, was for shot-receiver paths at 45 degrees to each of two principal directions and contained within the principal plane thereby subtended. Such records correspond to relatively far-offset shots (angle of incidence = 45 degrees) along profiles lying in principal directions.

This paper presents the results of some laboratory experiments (Figure 1) in which further shot records have been modelled for a wide range of offsets and for two fundamentally different profile orientations: a) along principal directions, for which the sagittal (or propagation) planes are principal planes, and b) at 45 degrees to two principal directions, for which the sagittal planes are no longer principal planes. For this latter case

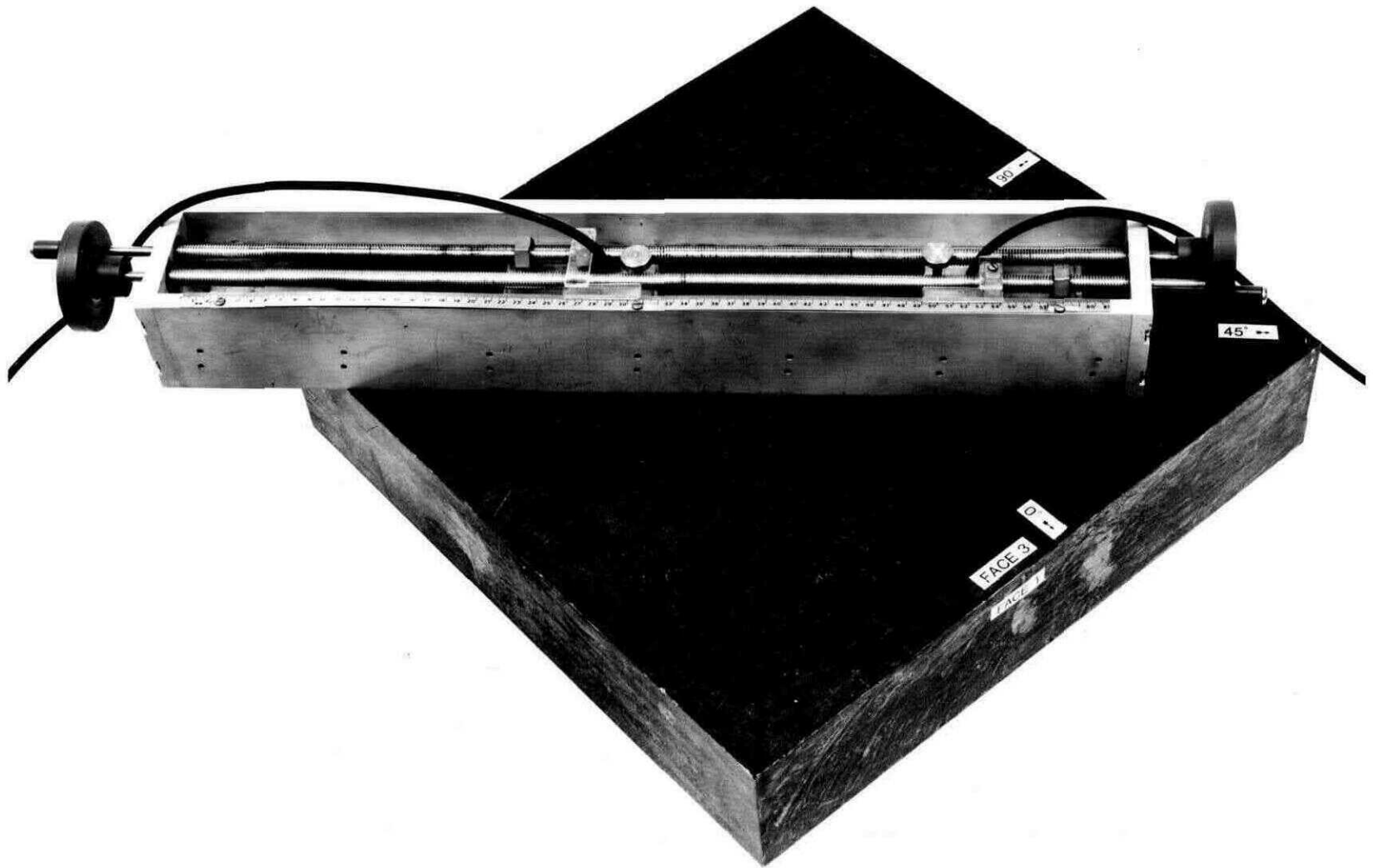


Fig. 1. Photograph of a slab of Phenolic CE with the experimental arrangement used in reflection experiments, i.e. with source and receiver transducers on the same surface of the slab. For the transmission experiments of this paper, the source and receiver transducers were placed on opposite surfaces.

we are reporting our first experimental results for cases where the propagation paths contain components of all three principal directions. Our earlier experiments (as well as some reported upon in this paper) for propagation within symmetry planes did not fully utilize the orthorhombic nature of the phenolic and only yielded results that could have been obtained in media of hexagonal symmetry (transverse isotropy). Such experimental results obtained on synthetic materials have been reported by Ebram et al. (1990) and Rathore et al. (1990), among others. Similar laboratory experiments using ultrasonic waves on real rock samples have been carried out by Jones and Wang (1981), Lin (1985) and Sayers (1988, 1990), for example. However, we are not aware of any other published results of the kind reported here of physical seismic modelling in orthorhombic materials.

We document our results in two related areas, the variation of NMO (or stacking) velocity with offset and analysis of the shot records obtained for the nine different combinations of shot and receiver polarization (vertical, radial, transverse). In both these areas, we carried out transmission experiments in which the source and receiver transducers were on opposite sides of the phenolic slab (Figure 1). This reduced the number of unwanted arrivals that would have accompanied reflection experiments with both transducers on the same surface (as pictured in Figure 1).

VARIATION OF VELOCITY WITH ANGLE OF INCIDENCE

The variation of velocity (group and phase) with direction of propagation is the fundamental property of seismic anisotropy from which all other manifestations, such as shear-wave splitting and wave-surface singularities, ensue. The actual directional dependence of velocities for various symmetries has been studied by Backus (1965), Crampin (1977) and Crampin and Kirkwood (1981), for example. The specific dependence of NMO or stacking velocity upon angle of incidence (or offset) has been examined by Levin (1979), Thomsen (1986) and Uren (1989), among others. Although the exact expressions for seismic velocities as functions of direction are very complicated and not easily manipulated, approximate expressions have been presented by Backus (1965), Crampin (1977) and Thomsen (1986) for cases in which the anisotropy is weak. Such approximate expressions are particularly appropriate for transverse isotropy (hexagonal symmetry) but also provide good estimates of the velocity variations in symmetry planes for all symmetry systems (Crampin and Kirkwood, 1981), in particular for the present case of orthorhombic symmetry.

The measures of anisotropy as formulated in three parameters by Thomsen (1986) have been discussed in Paper 1 and evaluated for our Phenolic CE for each of the three symmetry planes (Paper 1, Table 2). With these values, it is a straightforward exercise to apply the approximate expressions for phase-velocity as a function of angle of incidence, as presented by Thomsen (1986, equations 16), to obtain approximate theoretical estimates of the variations in the principal planes of the qP and qSH phase velocities. These equations are:

$$v_P(\theta) = v_P(0) (1 + \delta \sin^2 \theta \cos^2 \theta + \epsilon \sin^4 \theta)$$

and

$$v_{SH}(\theta) = v_{SH}(0) (1 + \gamma \sin^2 \theta).$$

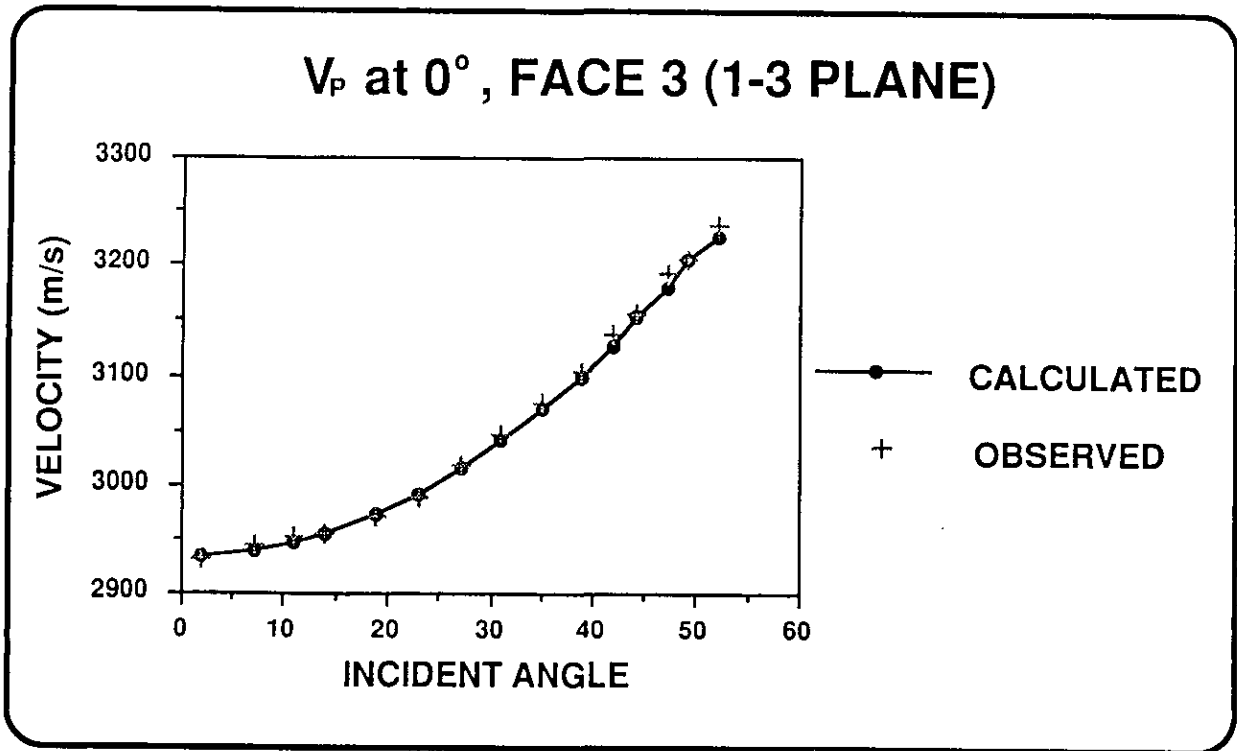


Fig. 2. Variation of qP velocity with angle of incidence for a profile in the 1-direction as *observed* in the phenolic and *calculated* from Thomsen's (1986) equations.

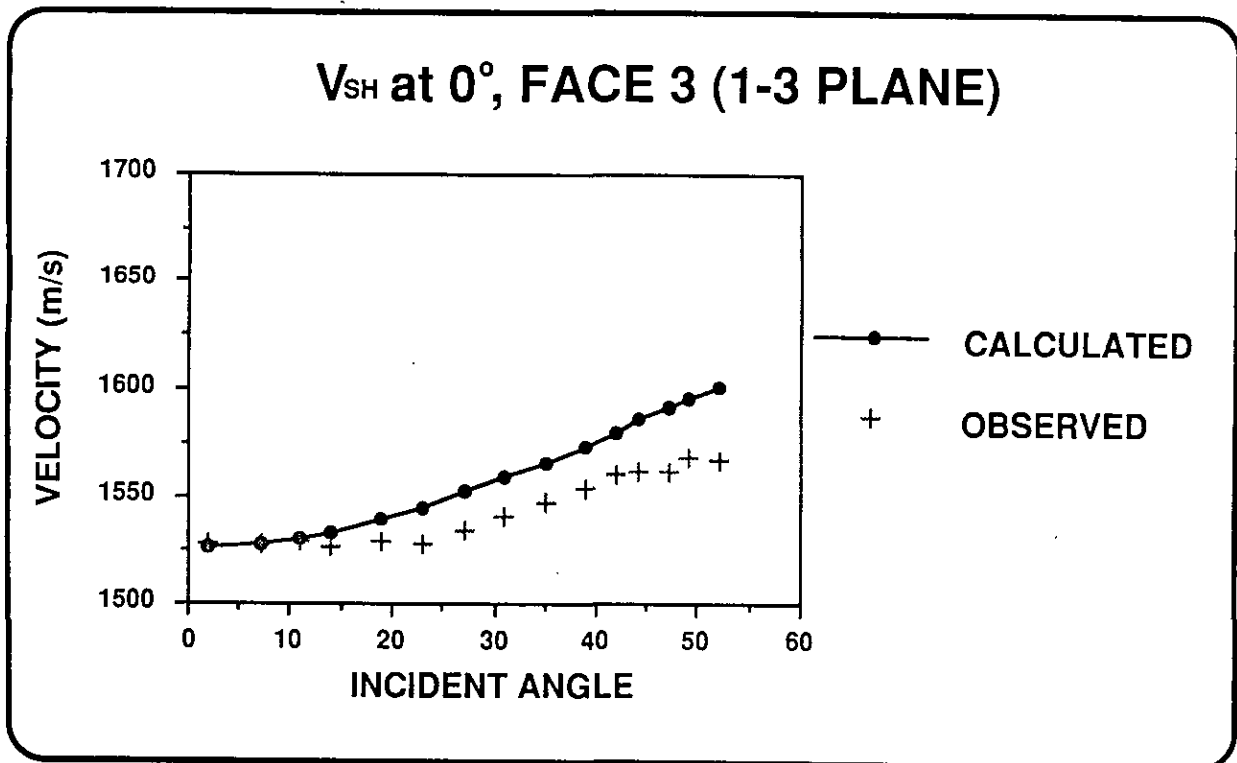


Fig. 3. As Figure 2 for qSH and a profile in the 1-direction.

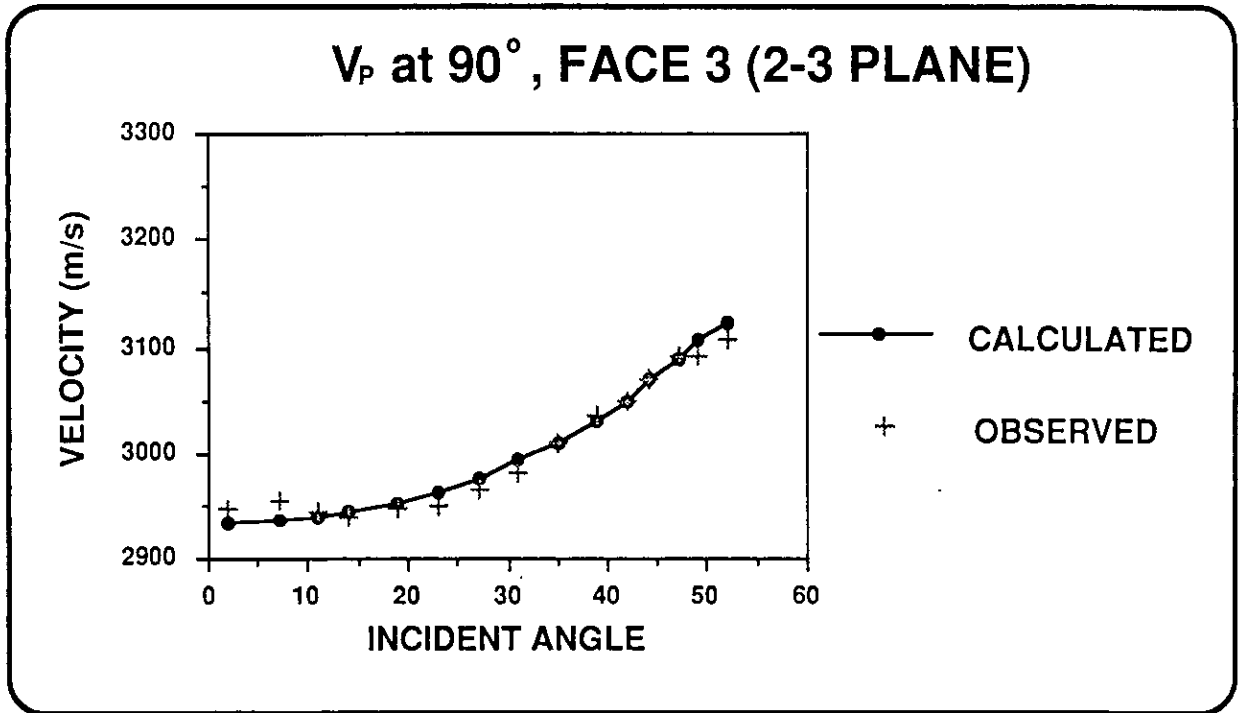


Fig. 4. As Figure 2 for qP and a profile in the 2-direction.

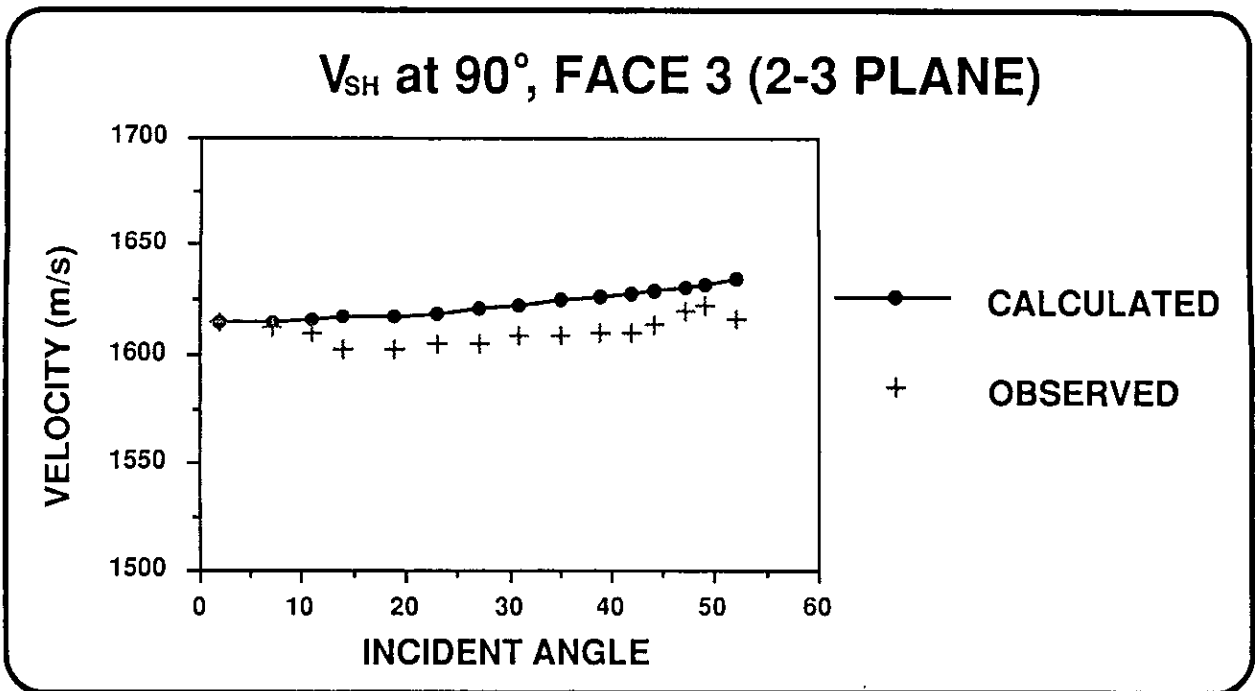


Fig. 5. As Figure 2 for qSH and a profile in the 2-direction.

In addition, it has been shown by Backus (1965) and Thomsen (1986) that for weakly anisotropic media, group velocities (i.e. the ray velocities that we measure) and phase velocities (calculated from the above equations) are approximately equal.

With the experimental arrangement shown in Figure 1, except that we placed sources and receivers on opposite sides of the slab, we measured group traveltimes versus offset. In Figures 2 to 5 we have plotted for comparison the NMO velocities that we have thus determined and those calculated from the approximate expressions of Thomsen (1986). This has been done for the qP and qSH waves propagating in the two "vertical" planes 1-3 and 2-3 (taking the 3-axis in the phenolic, the one perpendicular to the lamination, as the vertical). We did not carry this out for qSV waves because the shear-wave window, discussed further in the next section, did not extend to sufficiently far offsets.

In order to determine experimentally the variation of these NMO velocities with direction (angle of incidence) a correction had to be applied. For any particular source-receiver offset, for which a travelttime measurement has been made, an initial path length and angle of incidence are determined from basic trigonometry. In doing this, the source and receiver "points" are taken to be the centres of the respective transducers. Preliminary calculations showed us that the effective path length was in fact shorter than the nominal distance between transducer centres and was perhaps more like the distance between nearest edges of transducers which, for our scaled distances, constituted a significant difference. (The transducer diameter of 12.5 mm scales up to 62.5 m at 1:5000.) The correction was determined as follows. We repeated the shot profile with the very same geometry and the same thickness of material, except that we used an isotropic medium. The variations in travelttime with offset for this material were entirely due to geometry, with no anisotropic contribution. We were therefore able, on the basis of measured travelttimes and a known (invariant) velocity to determine an effective path length, and thus incidence angle, for each nominal source-receiver offset. This empirical correction was calculated and applied independently for each of the P and S transducer types.

Figures 2 to 5 show that the agreement between the experimentally determined NMO velocities and those calculated from the equations of Thomsen (1986) is better for the qP-wave velocity (significantly less than 1%) than for qSH (up to about 2%). This might be partly due to the fact that the particle motion for qSH waves is transverse to the symmetry plane. Most of the discrepancy for the qSH cases (Figures 3 and 5) seems to be associated with a curious decrease in velocity with offset before the increase, which we would have expected to occur monotonically from zero offset. In any event, the error in the qSH case is only about 1% on average and is exaggerated by the scaling of Figures 3 and 5. These results show that, in the principal planes of the phenolic, the measured anisotropies of up to 22% and 10% (for P and S, respectively) may still be loosely classified as weak, in line with Thomsen's stated range of 10 to 20% for weak anisotropy.

ANALYSIS OF THE VECTOR WAVEFIELD GENERATED BY MULTICOMPONENT SOURCES

The physical modelling capability described in the preceding sections has also been applied to generate several shot records along different profiles on the 3-face (taken as horizontal) of the phenolic slab (Figure 1). Profiles have been shot at 0 degrees (the 1-direction), 45 degrees and 90 degrees (the 2-direction) and, in general, records have been acquired for nine different combinations of shot and receiver polarizations.

Once again, these are transmission experiments with source and receiver transducers on opposite sides of a slab of the phenolic material. Figure 6 illustrates this and also shows how a compressional head wave will be generated at the critical angle. For the

corresponding critical offset and beyond, the shear-wave arrivals will suffer interference from this head wave. This critical distance defines the limits of the so called shear-wave window. One would expect the polarization of the compressional head wave to be within the sagittal plane and perhaps closer to horizontal than vertical. So we might expect it to be strongest on radial-receiver records and weakest on transverse-receiver records. However, these conventional (isotropic) expectations must be applied with caution, if not skepticism, in the anisotropic case.

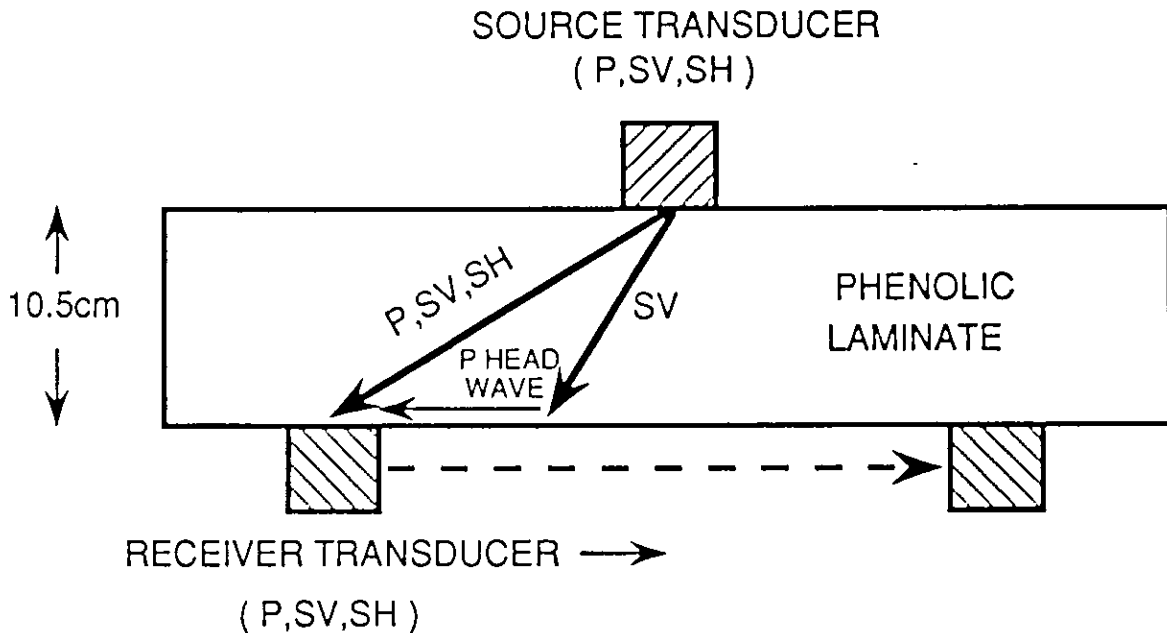


Fig. 6. Schematic diagram of wave propagation paths and transmission-experiment design as seen in section.

For the 0-degree and 90-degree records (Figures 7 to 10) there is sagittal symmetry (i.e. the sagittal planes are symmetry planes) and one does not observe any wave phenomena in the records that could not have been seen for a transversely isotropic medium. In these figures, only the vertical-vertical (V-V: vertical-source, vertical-receiver) record (Figure 8) is shown for the 90-degree profile as these records are very similar in nature to the 0-degree records (Figures 7, 9 and 10). Arrows labelled V_v indicate where onsets would have occurred had the vertical-path (zero-offset) velocity persisted isotropically out to the greatest offset. Arrows marked V_h show where these onsets would have come on the far trace if the horizontal-path velocity (in the profile direction) obtained isotropically.

The effect of the shear-wave window is seen in Figures 7 to 9 where the SV-P conversion at the base of the slab (Figure 6) arrives before and interferes with the SV phase. Note that this head wave has greater amplitude on the radial-radial (R-R) record (Figure 9) because the polarization of this compressional wave is nearly horizontal. So, outside the shear-wave window (from roughly -250 to 250 m on this scaled section) the P head wave

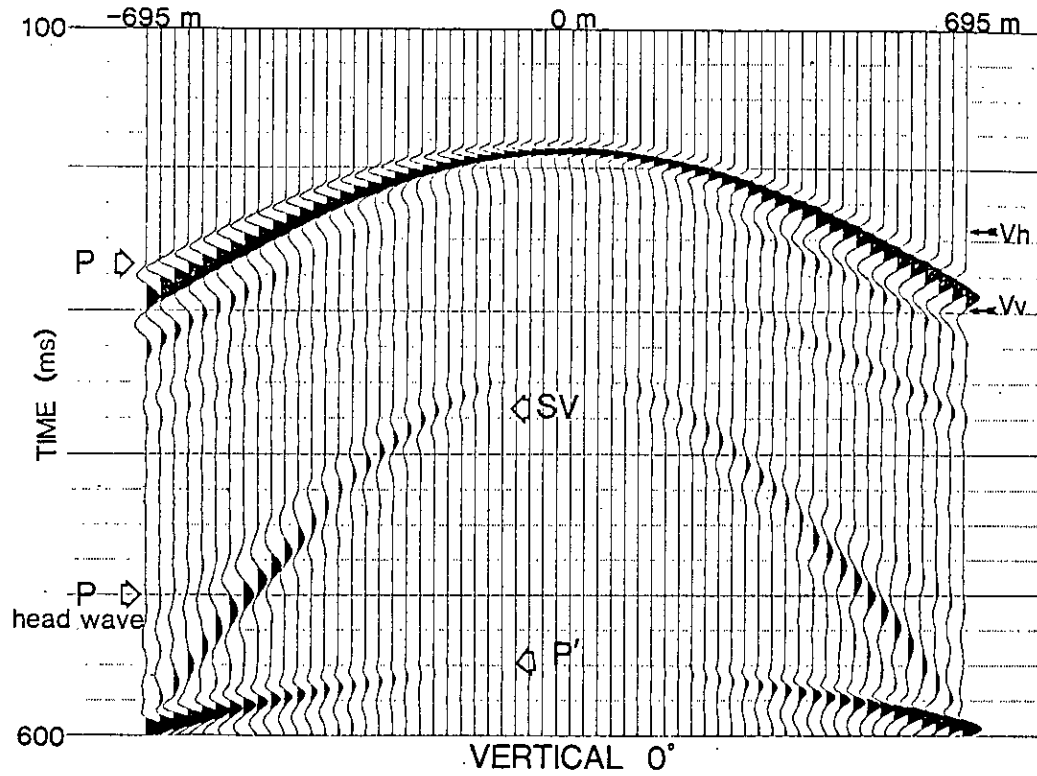


Fig. 7. Shot record for a profile in the 1-direction with vertically polarized source and receiver transducers (V-V); distances and times scaled by a factor of 5000.

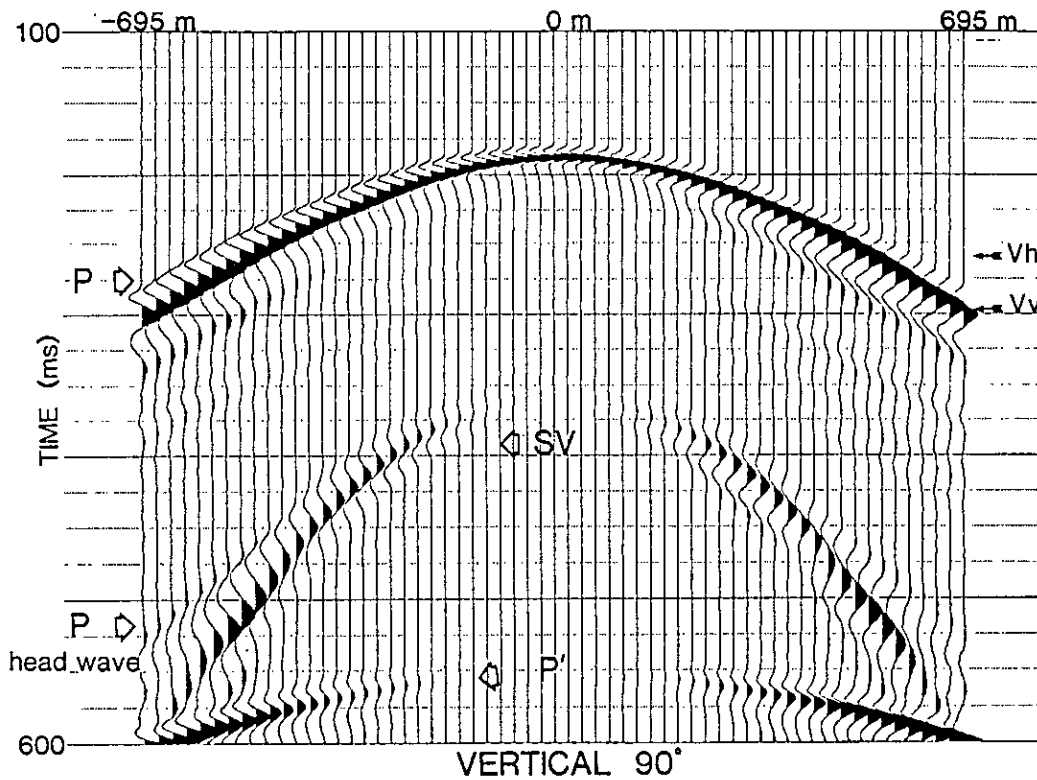


Fig. 8. As Figure 7 for a profile in the 2-direction.

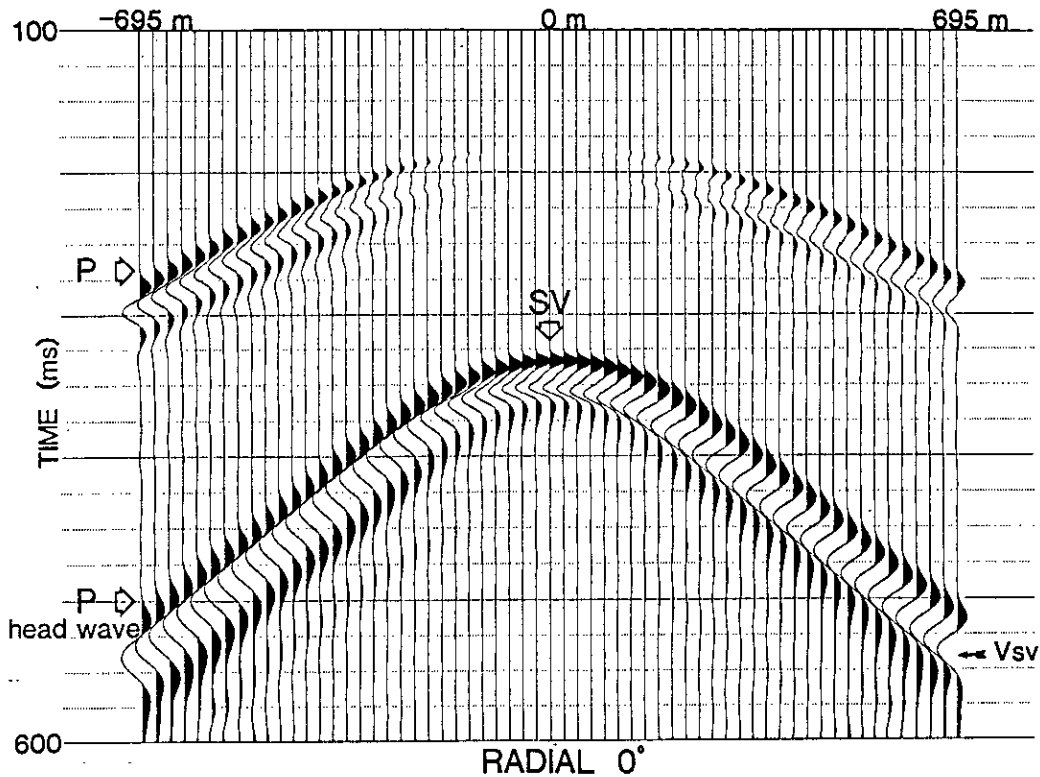


Fig. 9. As Figure 7 for radially polarized source and receiver (R-R).

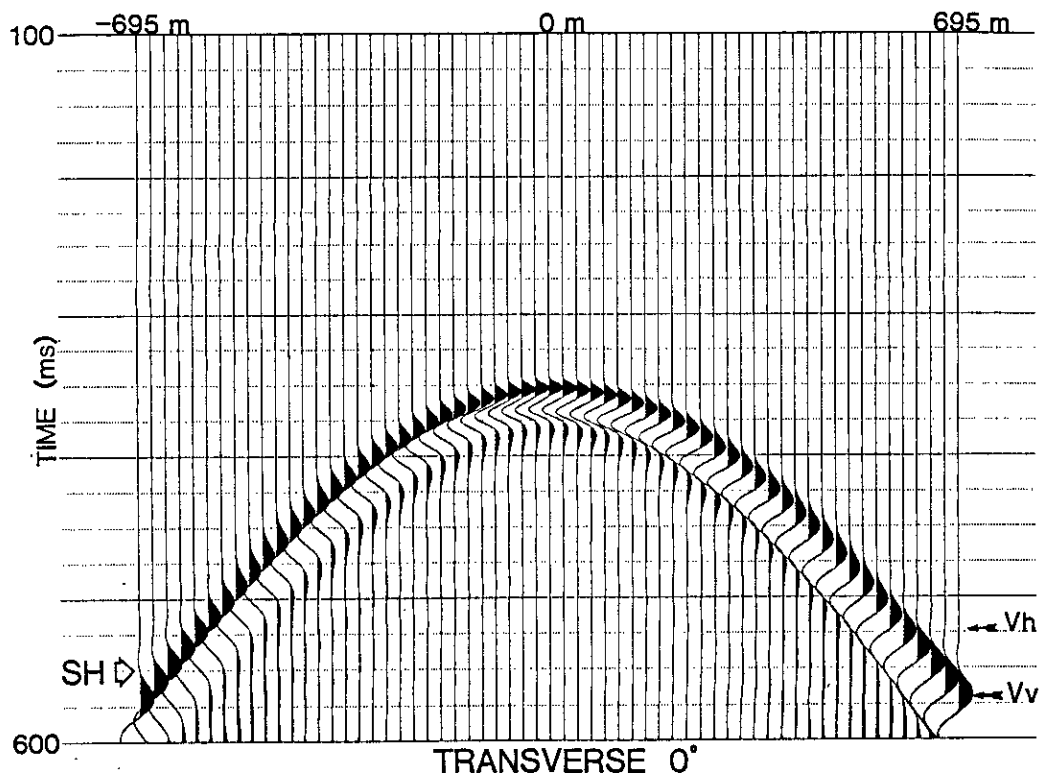


Fig. 10. As Figure 7 for transversely polarized source and receiver (T-T).

totally obscures the SV. On the V-V sections (Figures 7 and 8) the interference is apparently not nearly as great but the picking of accurate SV-onset times is still made practically impossible. For the T-T case (Figure 10) the "walls" surrounding the shear-wave window are transparent because of the polarizations of source and receiver and because of the sagittal symmetry. The fact that these are transmission and not reflection records probably also contributes to their simplicity of appearance.

In Figures 11 and 12, records acquired along 45-degree profiles are shown, the first of them an R-R record and the second a T-T record. In these we observe effects, not seen in the 0-degree or 90-degree records, that give a hint of the complexity of wave propagation in off-symmetry planes for an orthorhombic medium. In both of these shot records (Figures 11 and 12), split shear waves are clearly visible on the zero-offset traces (identical on the two sections) and for the nearest offsets. However, as offset increases, one of the qS arrivals dies out: the qS1 on the R-R record and the qS2 on the T-T record. This effect could conceivably be caused by cusping on complex wave surfaces, by rotations of polarizations into the plane perpendicular to the particular receiver polarization of each record, or by a relative-amplitude effect wherein the phases in question do not actually die out but simply become very low-amplitude at larger offsets. (Note that each trace is true-relative-amplitude but traces have been manually scaled relative to each other simply to maintain a roughly constant dynamic range). The wave phenomena we observe could also be due to some combination of these three effects. All of these are related manifestations of the general complexities of shear-wave propagation in arbitrary anisotropic media, complexities which are most pronounced in the neighbourhood of cusps on the wave or group-velocity surfaces or of singularities on the slowness or phase-velocity surfaces.

Musgrave (1970) discusses these topics in some detail and shows a number of relatively simple wave and slowness surfaces in symmetry planes. The full extent of the complexities are, however, generally realized in off-symmetry planes. Dellinger and Etgen (1989) show a synthetic example, generated on the basis of a particular orthorhombic medium (namely, cracked Greenhorn shale), of wave surfaces in an off-symmetry plane (Figure 13). Crampin and Yedlin (1981) and Crampin (1985, 1989, 1990) discuss the topic of shear-wave singularities and show examples of the rapid fluctuations in amplitudes and polarizations near such singularities.

In order to try to get a better look at polarizations for a particular shot, we decided to shoot a full "nine-component" record. So, for example, instead of just recording with a transversely sensitive transducer in the case of the transverse source, we would also record with vertically and radially sensitive transducers; and so on for all three source transducers. These results are shown in Figures 14 to 18.

Due to the fact that it can be difficult to replicate the source pulses in different experiments run at intervals of days or more, but not too difficult to maintain source-pulse form over an experiment of a few hours or so, we decided to shoot all nine components as one experiment. Comparison of Figures 11 and 12 with the R-R and T-T panels of Figure 14 (shown expanded in Figures 15 and 18), shows that, although there are some differences in pulse shape and therefore some of the fine details on traces, the overall results in terms of wave phases present, traveltimes, etc., appear to be repeatable between experiments.

In Figures 15 and 16 the R-R and R-T records are shown enlarged. It can here be seen that the qS1 arrival that dies out on the radial-receiver record (R-R) persists to large offsets on the transverse-receiver record (R-T). This could be the result of a polarization rotation, perhaps near a singularity or, since we have not displayed true trace-to-trace relative amplitudes, the effect could be one of amplitude scaling.

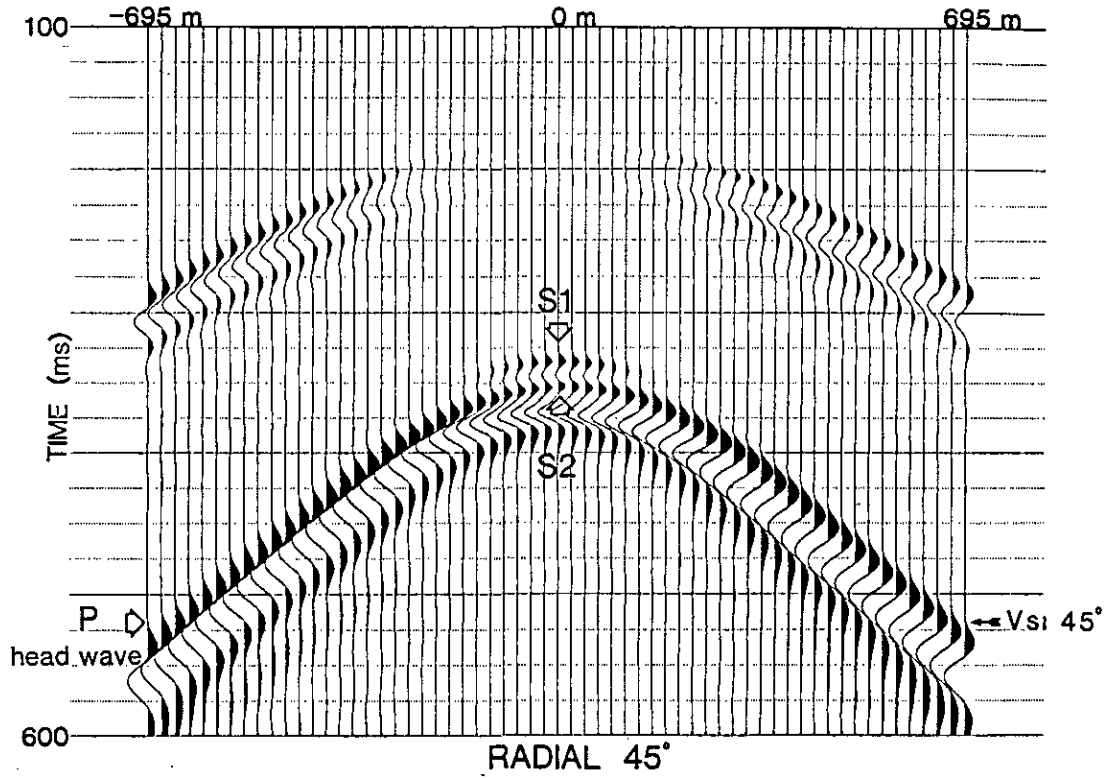


Fig. 11. As Figure 7 for a profile at 45 degrees to the 1- and 2-axes and R-R polarizations.

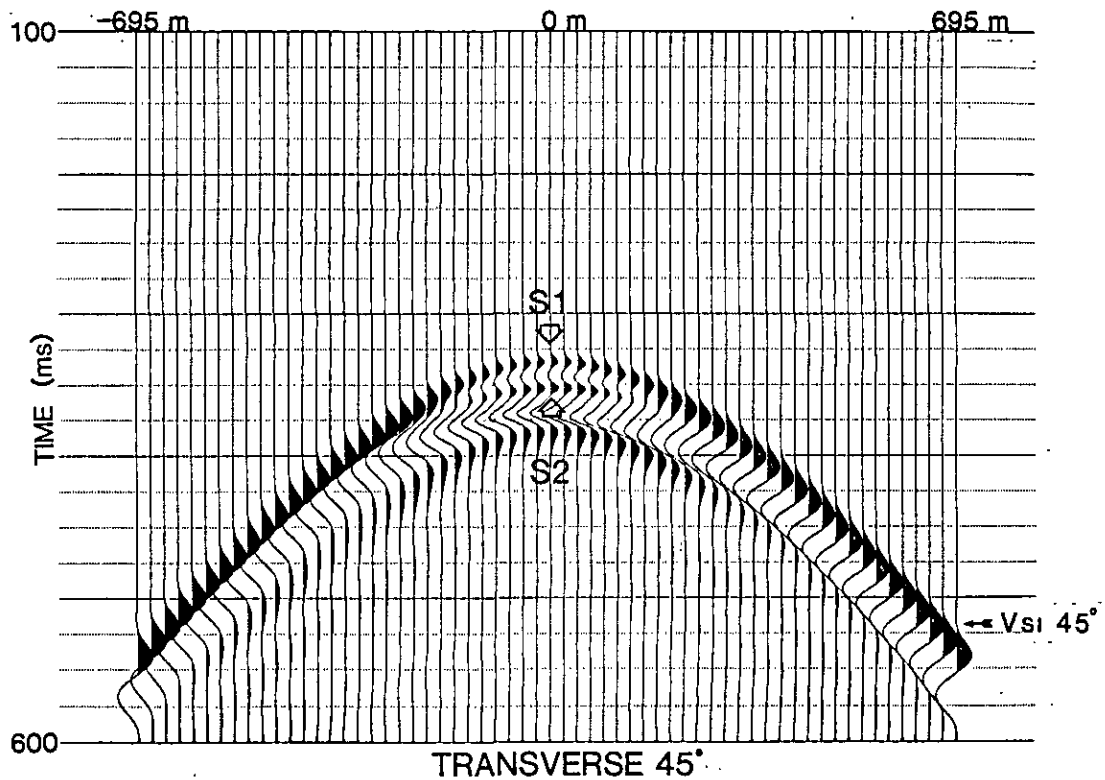


Fig. 12. As Figure 7 for a profile at 45 degrees to the 1- and 2-axes and T-T polarizations.

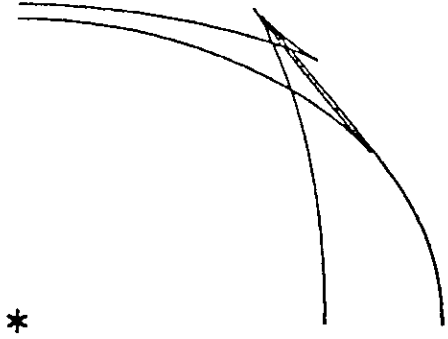


Fig. 13. Synthetic impulse response in an off-symmetry plane of an orthorhombic material numerically modelled as Greenhorn shale (Jones and Wang, 1981) with superposed cracks (from Dellinger and Etgen, 1989).

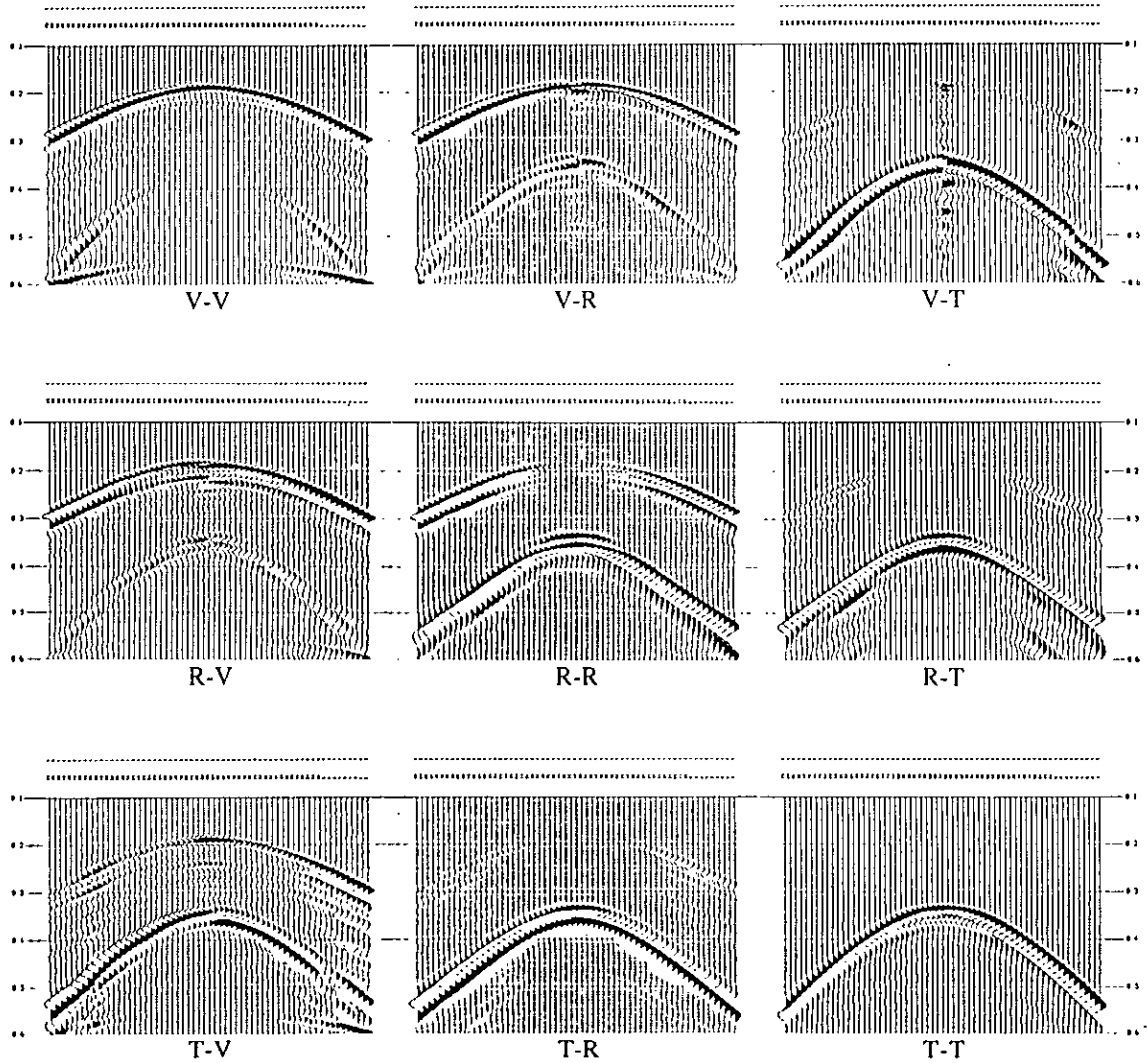


Fig. 14. Nine-component record for a profile at 45 degrees to the 1- and 2-axes, filtered at 5/10-100/200 Hz.

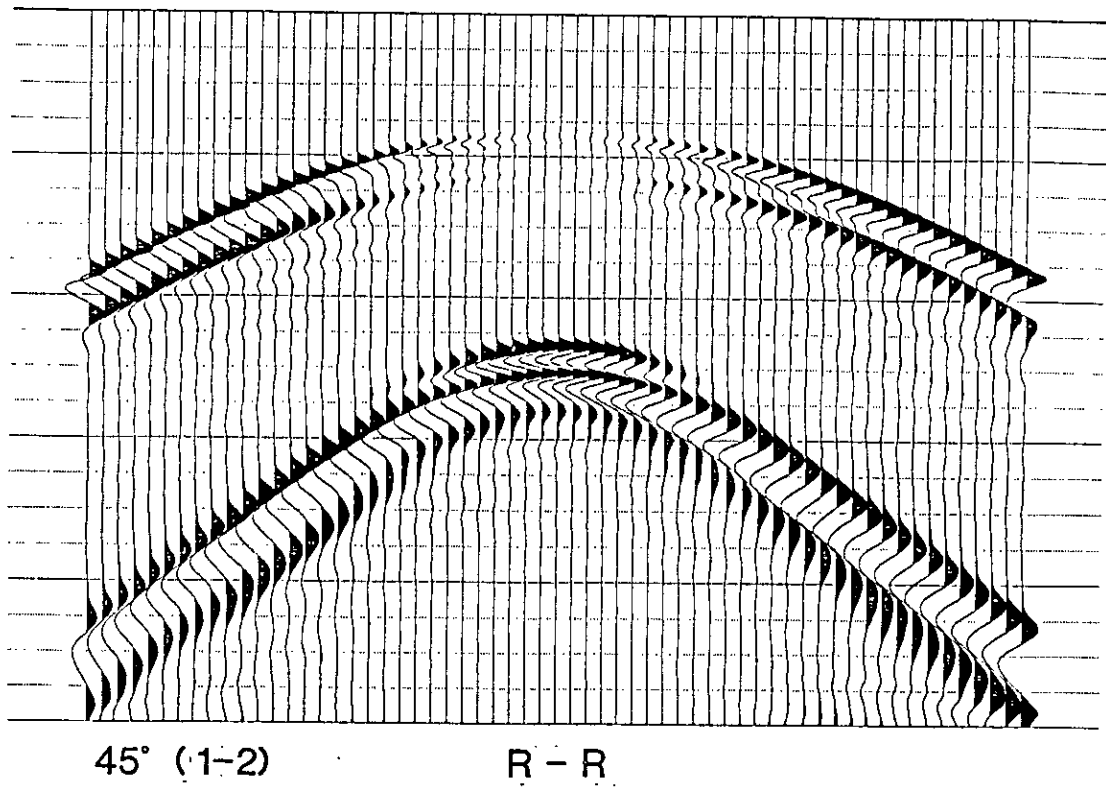


Fig. 15. Enlarged R-R component of Figure 14.

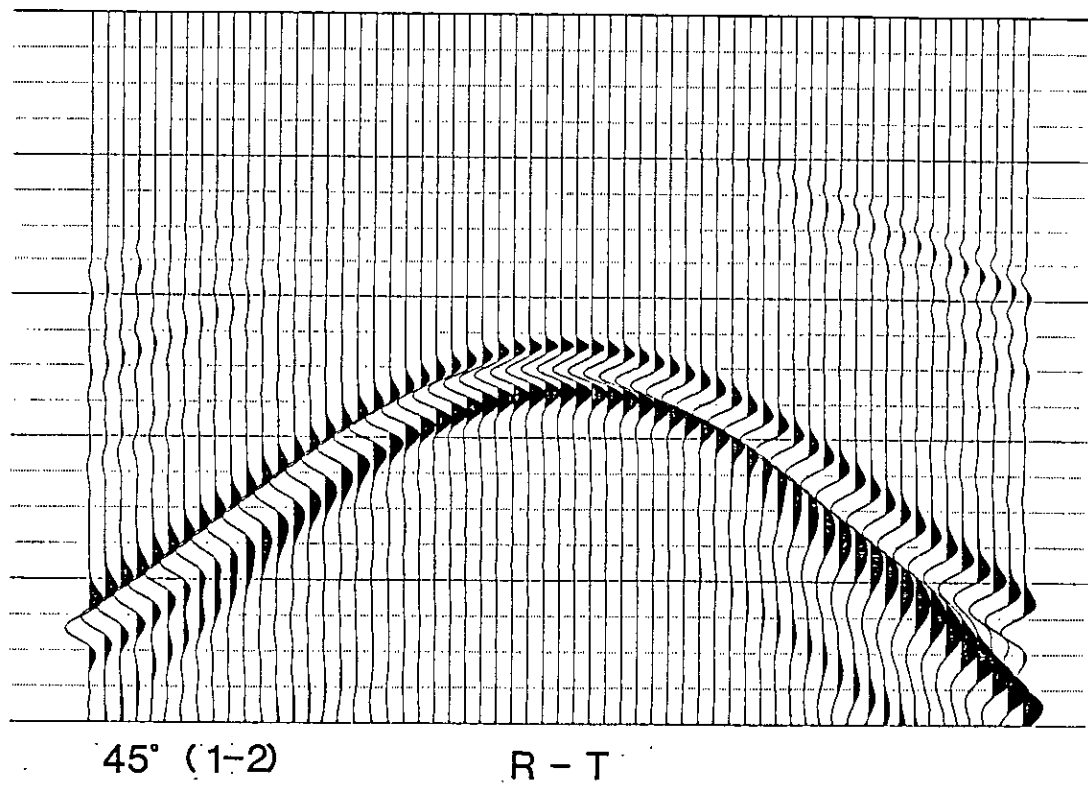


Fig. 16. Enlarged R-T component of Figure 14.

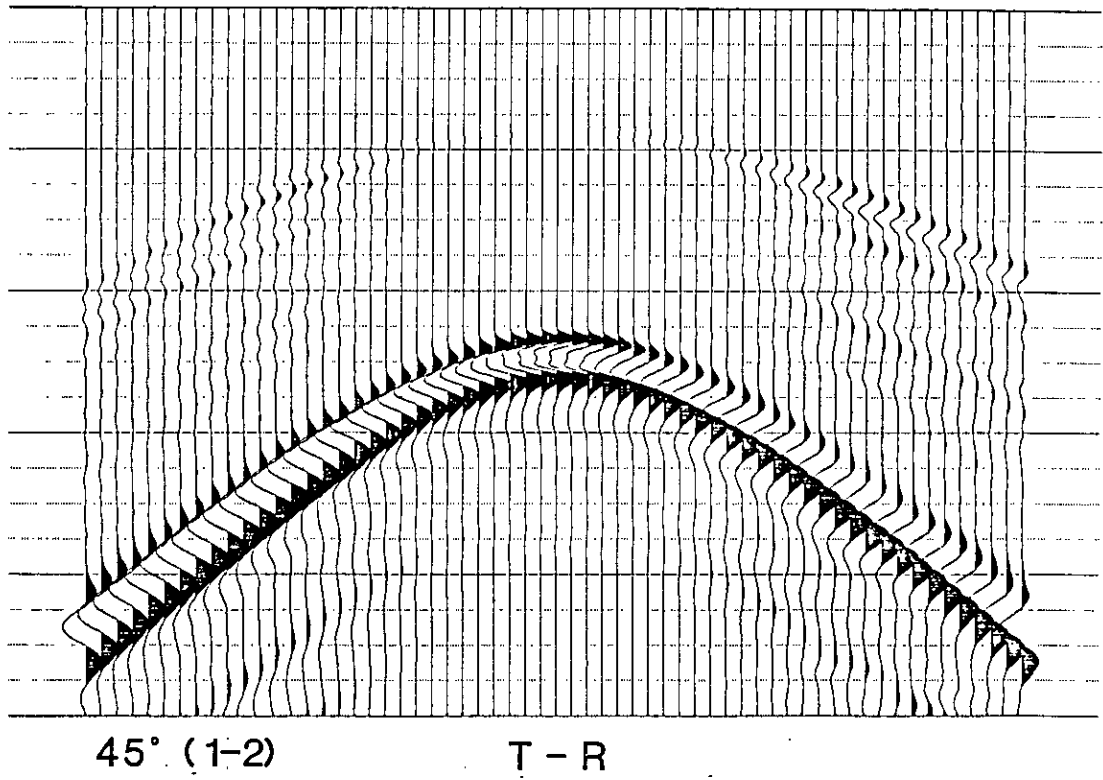


Fig. 17. Enlarged T-R component of Figure 14.

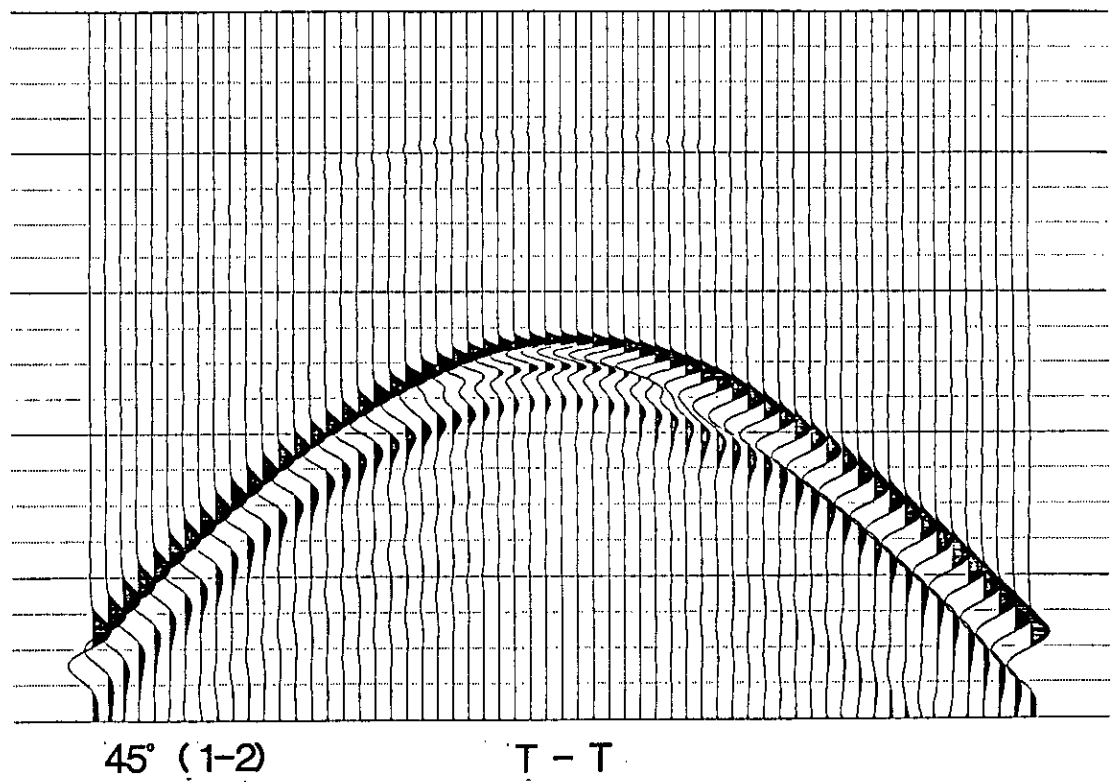


Fig. 18. Enlarged T-T component of Figure 14.

In Figures 17 and 18 the T-R and T-T records are enlarged. At first glance it appears as if the qS2 phase on the transverse-receiver record (T-T) is scarcely visible on the radial-receiver record (T-R) and that the same qS1 arrival dominates both records. However, the apparent onset times of these phases on the two records are not the same at far offsets: the qS1 seems to arrive later on the T-T record. In fact, the earlier onset on the T-R record probably represents compressional head-wave energy beyond the shear-wave window.

CONCLUSIONS AND FUTURE DIRECTIONS

We have verified that Thomsen's (1986) equations for qP- and qSH-wave velocities in transversely isotropic media are valid approximations in principal planes of our orthorhombic medium, at least within about 1% and 2%, respectively. On this basis we could say that our phenolic is still within the limits of weak anisotropy, even though the compressional and shear anisotropies are as much as 22% and 10%, respectively.

It has become clear to us in examining the full vector-wavefield records for even a weakly anisotropic medium with orthorhombic symmetry that it is extremely difficult to identify all wave phases and determine intuitively what sorts of propagation effects one is seeing when the sagittal plane is an off-symmetry plane. What we feel is needed then is to compare physical modelling results with synthetic seismograms and other theoretical results (e.g. positions of singularities) computed by means of full-waveform anisotropic numerical modelling. Only then, in our opinion, will it be possible to identify many of the complicated and rapidly (spatially) fluctuating effects that, for example, occur around singularities. Moreover, by making such comparisons for various numerical modelling algorithms based on different theoretical schemes, it may well be possible to determine which techniques are superior for the tasks at hand. We are now, therefore, pursuing collaborations with a number of groups who have developed these capabilities. In particular, we have received preliminary results from S. Crampin (British Geological Survey) of their ANISEIS software indicating the positions of shear-wave singularities in the phenolic. Some of our next laboratory experiments will entail the generation and recording of waves on raypaths close to the singular directions in order to observe what sorts of polarization and amplitude fluctuations actually occur. We are also awaiting results from J. Dellinger (Stanford University) of his wave-surface mapping program to gain some insight into what patterns of arrivals we might expect to see in different sagittal planes.

ACKNOWLEDGEMENTS

We are most grateful to the sponsors of the CREWES Project for their crucial financial support, to Dr. Rob Stewart for his scientific and moral support of this work and to Mr. Eric Gallant for his stalwart technical assistance.

REFERENCES

- Backus, G.E., 1965, Possible forms of seismic anisotropy of the uppermost mantle under oceans: *J. Geophys. Res.*, **70**, 3429-3439.
- Cheadle, S.P., Brown, R.J., and Lawton, D.C., 1990, Orthorhombic anisotropy: A physical model study: CREWES Rep., **2** (this volume).
- Crampin, S., 1977, A review of the effects of anisotropic layering on the propagation of seismic waves: *Geophys. J. Roy. Astr. Soc.*, **49**, 9-27.
- _____, 1985, Evaluation of anisotropy by shear-wave splitting: *Geophysics*, **50**, 142-152.
- _____, 1989, Suggestions for a consistent terminology for seismic anisotropy: *Geophys. Prosp.*, **37**, 753-770.
- _____, 1990, Effects of point singularities on shear-wave propagation in sedimentary basins: *Geophys. J. Internat.*, in press.

- Crampin, S., and Kirkwood, S.C., 1981, Velocity variations in systems of anisotropic symmetry: *J. Geophys.*, **49**, 35-42.
- Crampin, S., and Yedlin, M., 1981, Shear-wave singularities of wave propagation in anisotropic media: *J. Geophys.*, **49**, 43-46.
- Dellinger, J., and Etgen, J., 1989, Wave-type separation in 3-D anisotropic media: 59th Ann. Internat. Mtg., Soc. Expl. Geophys., Expanded Abstracts, 977-979.
- Ebrom, D.A., Tatham, R.H., Sekharan, K.K., McDonald, J.A., and Gardner, G.H.F., 1990, Hyperbolic travelttime analysis of first arrivals in an azimuthally anisotropic medium: A physical modeling study: *Geophysics*, **55**, 185-191.
- Jones, E.A., and Wang, H.F., 1981, Ultrasonic velocities in Cretaceous shales from the Williston basin: *Geophysics*, **46**, 288-297.
- Levin, F.K., 1979, Seismic velocities in transversely isotropic media: *Geophysics*, **44**, 918-936.
- Lin, W., 1985, Ultrasonic velocities and dynamic elastic moduli of Mesaverde rock: Lawrence Livermore Nat. Lab. Rep. 20273, rev. 1.
- Musgrave, M.J.P., 1970, *Crystal acoustics*: Holden-Day.
- Rathore, J.S., Fjaer, E., Holt, R.M., and Renlie, L., 1990, Acoustic anisotropy of synthetics with controlled crack geometries: presented at 4th Internat. Workshop Seismic Anisotropy, July 2-6, Edinburgh.
- Sayers, C.M., 1988, Stress-induced ultrasonic wave velocity anisotropy in fractured rock: *Ultrasonics*, **26**, 311-317.
- _____, 1990, Ultrasonic studies of deformation and failure of rocks: *in* Datta, S.K., Achenbach, J.D., and Rajapakse, Y.S., Eds., *Elastic waves and ultrasonic nondestructive evaluation*, Elsevier Sci. Publ.
- Thomsen, L., 1986, Weak elastic anisotropy: *Geophysics*, **51**, 1954-1966.
- Uren, N.F., 1989, Processing of seismic data in the presence of elliptical anisotropy: Ph.D. thesis, Univ. of Houston.